NASA TM X-130

TECHNICAL MEMORANDUM
X-130

LONGITUDINAL AERODYNAMIC CHARACTERISTICS OF A WING-BODY-TAIL MODEL HAVING A HIGHLY TAPERED, CAMBERED 45° SWEPT WING OF ASPECT RATIO 4 AT TRANSONIC SPEEDS

By F. E. West, Jr.

Langley Research Center
Langley Field, Va.

November 1959
Declassified October 1, 1961

NATIONAL AERONAUTICS AND SPACE ADMINISTRATION
WASHINGTON

NATIONAL AERONAUTICS AND SPACE ADMINISTRATION

TECHNICAL MEMORANDUM X-130

LONGITUDINAL AERODYNAMIC CHARACTERISTICS OF A WING-BODY-TAIL MODEL HAVING A HIGHLY TAPERED, CAMBERED 45° SWEPT WING OF ASPECT RATIO 4 AT TRANSONIC SPEEDS

By F. E. West, Jr.

SUMMARY

The longitudinal aerodynamic characteristics of a wing—body—horizontal-tail configuration designed for efficient performance at transonic speeds has been investigated at Mach numbers from 0.80 to 1.03 in the Langley 16-foot transonic tunnel. The effect of adding an outboard leading-edge chord-extension to the highly tapered 45° swept wing was also obtained. The average Reynolds number for this investigation was 6.7×10^6 based on the wing mean aerodynamic chord.

The relatively low tail placement as well as the addition of a chord-extension achieved some alleviation of the pitchup tendencies of the wing-fuselage configuration. The maximum trimmed lift-drag ratio was 16.5 up to a Mach number of 0.9, with the moment center located at the quarter-chord point of the mean aerodynamic chord. For the untrimmed case, the maximum lift-drag ratio was approximately 19.5 up to a Mach number of 0.9.

INTRODUCTION

Long-range airplanes designed for flight at transonic and low supersonic speeds should have wings with high aspect ratios, large angles of sweep, and low thickness-chord ratios. For configurations without devices on the wing, the maximum aspect ratio at a given sweep angle for which satisfactory longitudinal stability characteristics can be obtained through the lift range is unfortunately limited. The limitations are particularly restrictive at transonic speeds where wing flow separation

is caused by shocks which extend laterally across the upper surface of the wing. (See ref. 1.) Evidence of this flow separation, which causes unstable pitching-moment changes at moderate lift, initially occurs behind the shocks on the outboard wing sections. Reference 1 indicates that reducing the wing area behind the shocks should alleviate the unstable pitching-moment changes. One possible method of reducing this wing area would be to reduce the wing taper ratio.

The wing of the configuration for which data are presented in this paper combines the desirable low taper ratio and high sweep with a moderate amount of wing camber. These design features have been incorporated in a model which employs area-rule considerations to increase efficiency at the high subsonic cruise and supersonic dash conditions. The wing has 45° sweep, an aspect ratio of 4, a taper ratio of 0.15, and thickness-chord ratios that vary from 6 percent at the root to 3 percent over the outboard 50 percent of the wing semispan.

Force and loads data for a geometrically similar wing have been published in references 2 and 3. The present data supplement this information to include the longitudinal aerodynamic characteristics with a horizontal tail and a leading-edge chord-extension. The results of this study were obtained in the Langley 16-foot transonic tunnel at Mach numbers from 0.80 to 1.03 and angles of attack up to about 19°.

SYMBOLS

a	airfoil mean-line designation; fraction of chord from leading edge over which design load is uniform
b	wing span
c	basic-wing local chord (parallel to plane of symmetry)
$\bar{c}$	basic-wing mean aerodynamic chord (parallel to plane of symmetry)
$\bar{c}_t$	horizontal-tail mean aerodynamic chord (parallel to plane of symmetry)
C_D	drag coefficient, Drag/qS
C_L	lift coefficient, Lift/qS
C_m	pitching-moment coefficient about quarter-chord point of $\bar{c}$, Pitching moment/qS$\bar{c}$

L/D	lift-drag ratio
l	distance from $0.25\bar{c}$ to $0.25\bar{c}_t$, measured with $i_t = 0^\circ$
M	free-stream Mach number
q	free-stream dynamic pressure
S	basic-wing area
S_t	horizontal-tail area
V	tail volume coefficient, $\frac{l}{\bar{c}} \frac{S_t}{S}$
x_b	body station, distance from nose of body
y_b	body local radius or one-half of body local width
z_b	one-half of body local height
z	perpendicular distance between wing and tail chord planes, measured with $i_t = 0^\circ$, negative when tail chord plane is below wing chord plane
α	angle of attack of body center line
ϵ	effective downwash angle at horizontal tail
i_t	horizontal-tail incidence referred to body center line
C_{L_α}	lift-curve slope
$\frac{\partial C_m}{\partial C_L}$	static-longitudinal-stability parameter
$C_{m_{i_t}}$	horizontal-tail effectiveness parameter
$\frac{\partial \epsilon}{\partial \alpha}$	downwash-angle parameter

Subscripts:

max maximum

min minimum

APPARATUS

The investigation was made in the Langley 16-foot transonic tunnel. The air-flow and power characteristics of this tunnel are presented in reference 4.

Dimensional details of the model are given in figure 1, and a photograph of the model installed in the tunnel is shown in figure 2. As shown in the photograph, no vertical tail was used in the investigation. The external dimensions of the wing-body combination are generally proportional to those of a smaller wing-body combination shown in references 2 and 3. The scale factor between the two models is 2.408. Except for an elliptical cross section downstream of $x_b = 66$ inches, a slightly longer afterbody, and small increases in cross-sectional area beginning at $x_b = 73.125$ inches, the body dimensions are proportional to those for the model shown in references 2 and 3. All wing dimensions of the two models are proportional.

The steel wing had 45° sweep of the quarter-chord line, an aspect ratio of 4, and a taper ratio of 0.15. The wing section was an NACA 64A206, $a = 0$ at the root (plane of symmetry), and varied linearly in thickness to an NACA 64A203, $a = 0.8$ (modified) over the outboard 50 percent of the semispan. Airfoil ordinates for the wing are available in reference 2.

The body consisted of steel except for a plastic forebody. The body was indented symmetrically for $M = 1.2$, had a fineness ratio of 12.6, and a ratio of body frontal area to wing area of 0.032. Body ordinates are given in table I.

A separate horizontal tail was made for each angle of incidence. The tail angles of incidence were 0.3°, -4.2°, -8.0°, and -11.9°. Each tail had 45° sweep of the quarter-chord line, an aspect ratio of 4, and a taper ratio of 0.6. Tail airfoil sections varied linearly in thickness from an NACA 64A006 section at the root (plane of symmetry) to an NACA 64A003 section at the tip. For these tails, which were made of plastic with steel cores, $S_t/S = 0.20$, $l/\bar{c} = 1.86$, $2z/b = 0.053$, and $V = 0.373$.

The leading-edge chord-extensions, which were made of steel, extended from 65 percent of the wing semispan to the wing tip. They had a constant chord equal to 15 percent of the wing chord at 65 percent of the wing semispan, except in the region of the rounded tip. The chord-extension sections corresponded to the forward projection of the wing sections along their chord lines. Between the maximum ordinates on a given surface for the projected chord-extension sections and the wing sections, the airfoil contour was parallel to the section chord lines.

Static forces and moments were measured on an internal strain-gage six-component balance. Four pressure orifices were located inside the body base for the measurement of base pressures.

TESTS

Six-component balance and base-pressure data were obtained for the various configurations at Mach numbers from 0.80 to 1.03 and usually angles of attack up to about 19°. The wing-body combination was tested without a horizontal tail and with horizontal tails at angles of incidence of 0.3°, -4.2°, -8.0°, and -11.9°. Leading-edge chord-extensions were tested on the model without a horizontal tail and with a horizontal tail at an angle of incidence of -4.2°.

The wing-body combination was also tested with boundary-layer transition strips located on the upper and lower surfaces of the wing and the body nose. The strips consisted of carborundum grains spread over a thin coating of shellac. The grains covered 5 to 10 percent of the strip areas. All strips had a width of 0.125 inch. Those on the wing began at 2.5 percent of the local wing chord, and the body strip began at 2.5 percent of the body length. Grain sizes used in the tests were No. 100 (nominal grain size of 0.006 inch) and No. 220 (nominal grain size of 0.003 inch). For these tests the angles of attack were limited to a range from -3° to 4°. Except where indicated, all data presented are for a transition-free condition.

The average Reynolds number (based on wing mean aerodynamic chord) for these tests varied from 6.5×10^6 at a Mach number of 0.80 to 6.8×10^6 at a Mach number of 1.03.

CORRECTIONS AND ACCURACIES

The lift and drag data have been adjusted to a condition of free-stream static pressure at the fuselage base. Except for the base-pressure

adjustments, sting-interference effects have been neglected. Tunnel-wall effects are small for the Mach number range of the present investigation (see ref. 5) and have also been neglected.

The accuracy of the aerodynamic coefficients based on balance precision and repeatability of data is believed to be within the following limits:

C_L	±0.01
C_D (at low angles of attack)	±0.001
C_D (at high angles of attack)	±0.004
C_m	±0.005

Angle-of-attack accuracy is estimated to be within ±0.1°.

RESULTS AND DISCUSSION

The longitudinal aerodynamic characteristics are presented in figure 3 for the basic configuration with the tail off and with the tail set at four angles of incidence. The effects of leading-edge chord-extensions on the longitudinal aerodynamic characteristics of the basic model without the tail and with the tail set at an angle of incidence of -4.2° are shown in figures 4 and 5, respectively. The variation of the longitudinal-stability parameter with lift coefficient for the configurations of figures 4 and 5 are shown in figure 6. The chord-extension achieved the expected alleviation (at $M = 0.80$ and 0.90) and delaying (at $M = 0.94$ and above) of the pitchup tendencies as shown by figures 5(c) and 6.

Small effects on the longitudinal aerodynamic characteristics may be noted in comparing the transition-off and transition-on curves of figure 7. Figure 8 which summarizes the effects of roughness shows that adding roughness caused small increases in minimum drag and a reduction of 1 to 2 in $(L/D)_{max}$ depending on the Mach number. Figure 8 also shows that only minor effects of roughness were noted on lift-curve slope.

The relatively low placement of the tail was dictated by a desire to alleviate the wing-body pitchup tendencies as much as practical. The stability characteristics shown in figure 3(c) indicate the expected improvement for such a placement. The effective downwash angles for this tail position, as obtained from the tail-on and tail-off pitching-moment

curves of figure 3(d), are presented in figure 9. A summary of the tail contribution to the stability characteristics is presented in figure 10. In this figure is shown the effect of Mach number on longitudinal stability, tail effectiveness, and downwash.

The maximum lift-drag ratios and lift coefficients at the maximum lift-drag ratios are summarized in figure 11. Trimming the complete model throughout the Mach number range resulted in an L/D penalty of between 3 and 4. However, this penalty would be much smaller if a more reasonable low-lift static margin had been chosen. The maximum trimmed L/D ratio was 16.5 up to a Mach number of 0.9 and dropped to 10 at a Mach number of 1.03. The maximum untrimmed L/D ratio was approximately 19.5 up to a Mach number of 0.9. The lift coefficient for maximum lift-drag ratio occurred approximately at the design value of 0.2 throughout the Mach number range, even for the trimmed model.

CONCLUSIONS

Results of an investigation at Mach numbers from 0.80 to 1.03 of the longitudinal aerodynamic characteristics of a wing-body-tail model having a highly tapered, cambered 45° swept wing of aspect ratio 4 with and without outboard leading-edge chord-extensions indicated the following:

1. Relatively low tail placement as well as addition of a chord-extension achieved some alleviation of the pitchup tendencies of the wing-fuselage configuration.

2. The maximum trimmed lift-drag ratio was 16.5 up to a Mach number of 0.9, with the moment center located at the quarter-chord point of the mean aerodynamic chord.

3. For the untrimmed case, the maximum lift-drag ratio was approximately 19.5 up to a Mach number of 0.9.

Langley Research Center,
National Aeronautics and Space Administration,
Langley Field, Va., July 30, 1959.

REFERENCES

1. West, F. E., Jr., and Henderson, James H.: Relationship of Flow Over a 45° Sweptback Wing With and Without Leading-Edge Chord-Extensions to Longitudinal Stability Characteristics at Mach Numbers From 0.60 to 1.03. NACA RM L53H18b, 1953.

2. Loving, Donald L.: A Transonic Investigation of Changing Indentation Design Mach Number on the Aerodynamic Characteristics of a 45° Sweptback-Wing—Body Combination Designed for High Performance. NACA RM L55J07, 1956.

3. Fischetti, Thomas L.: Investigation at Mach Numbers From 0.80 to 1.43 of Pressure and Load Distributions Over a Thin 45° Sweptback Highly Tapered Wing in Combination With Basic and Indented Bodies. NACA RM L57D29a, 1957.

4. Ward, Vernon G., Whitcomb, Charles F., and Pearson, Merwin D.: Air-Flow and Power Characteristics of the Langley 16-Foot Transonic Tunnel With Slotted Test Section. NACA RM L52E01, 1952.

5. Whitcomb, Charles F., and Osborne, Robert S.: An Experimental Investigation of Boundary Interference on Force and Moment Characteristics of Lifting Models in the Langley 16- and 8-Foot Transonic Tunnels. NACA RM L52L29, 1953.

TABLE I.- BODY ORDINATES

x_b, in.	y_b, in.	x_b, in.	y_b, in.	x_b, in.	y_b, in.	x_b, in.	y_b, in.	z_b,* in.
0	0	27.00	3.284	45.00	2.750	65.00	3.278	
.50	.210	28.00	3.338	46.00	2.720	66.00	3.255	3.255
.75	.284	29.00	3.388	47.00	2.712	68.00	3.177	3.215
1.00	.352	30.00	3.431	48.00	2.721	70.00	3.082	3.173
1.50	.475	31.00	3.461	49.00	2.754	73.125	2.852	3.108
2.00	.587	31.50	3.470	50.00	2.799	76.00	2.612	3.049
4.00	.972	32.00	3.471	51.00	2.852	78.00	2.440	3.008
6.00	1.296	32.50	3.470	52.00	2.912	80.00	2.261	2.967
8.00	1.582	33.00	3.464	54.00	3.041	82.00	2.083	2.926
10.00	1.838	33.50	3.456	56.00	3.186	84.00	1.907	2.884
12.00	2.074	34.00	3.443	57.00	3.250	86.00	1.722	2.841
14.00	2.284	35.00	3.405	58.00	3.288	87.50	1.586	2.812
16.00	2.478	36.00	3.354	59.00	3.311			
18.00	2.657	38.00	3.222	60.00	3.323			
20.00	2.818	40.00	3.068	61.00	3.325			
22.00	2.970	42.00	2.906	62.00	3.320			
24.00	3.108	43.00	2.844	63.00	3.309			
26.00	3.230	44.00	2.791	64.00	3.295			

*The value of z_b is equal to y_b for values of x_b not greater than 66.00 inches.

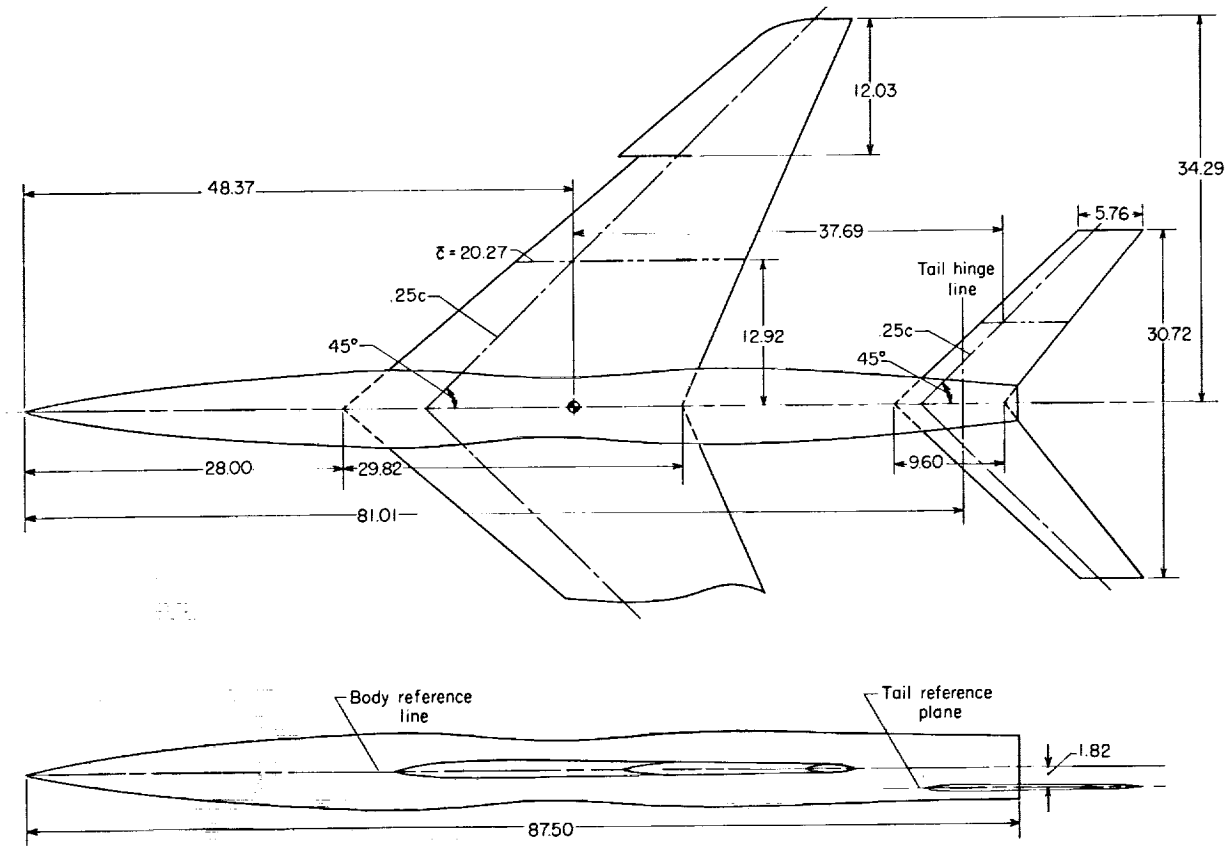

WING	HORIZONTAL TAIL
Sections ------- NACA 64A20X	Sections ------- NACA 64A00X
Area, ft^2 ------ 8.165	Area, ft^2 ------- 1.639
Aspect ratio---- 4	Aspect ratio---- 4
Taper ratio----- 0.15	Taper ratio----- 0.60
Sweep, c/4----- 45°	Sweep, c/4----- 45°

Figure 1.- Details of model. All dimensions are in inches.

Figure 2.- Photograph of model installed for tests. L-94598

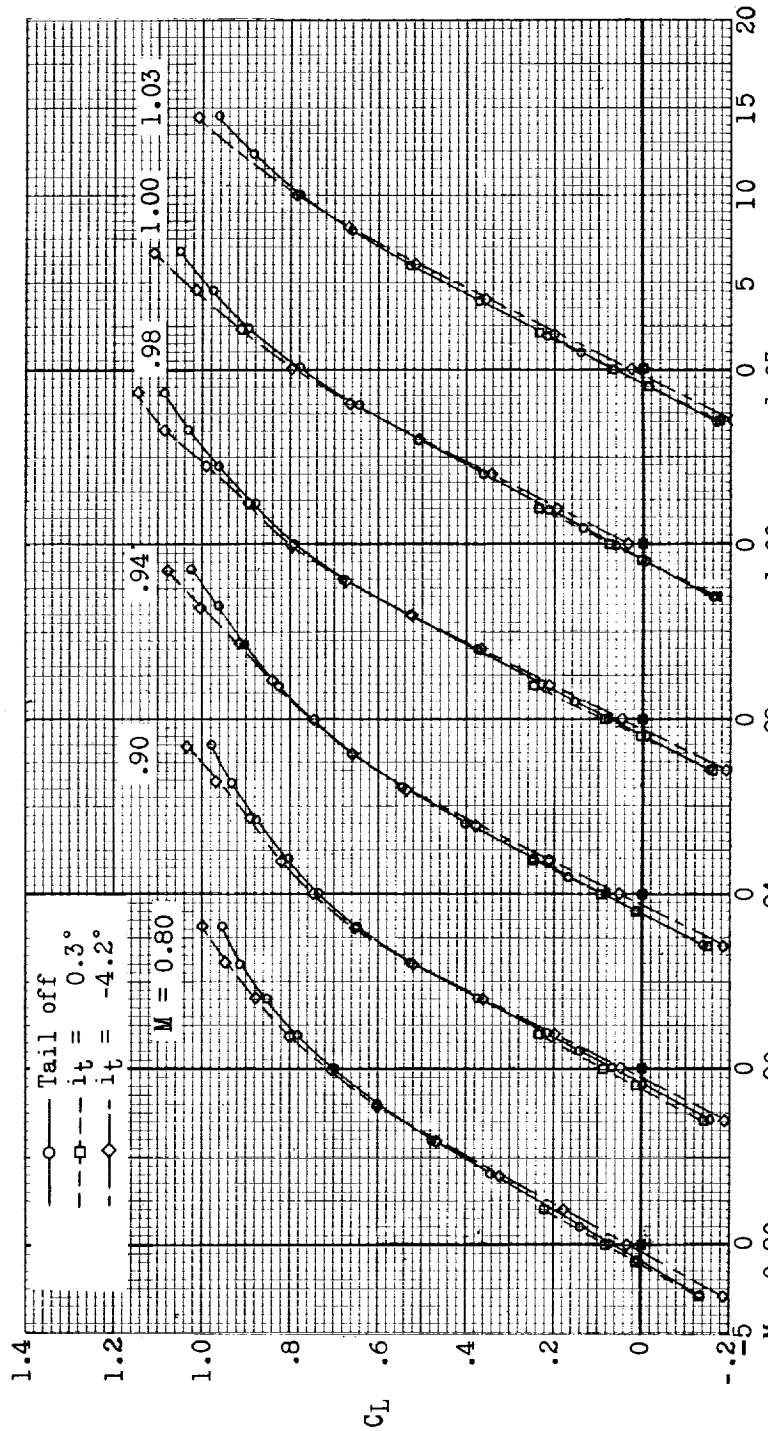

(a) Variation of C_L with α.

Figure 3.- Longitudinal aerodynamic characteristics for basic tail-off and tail-on configurations.

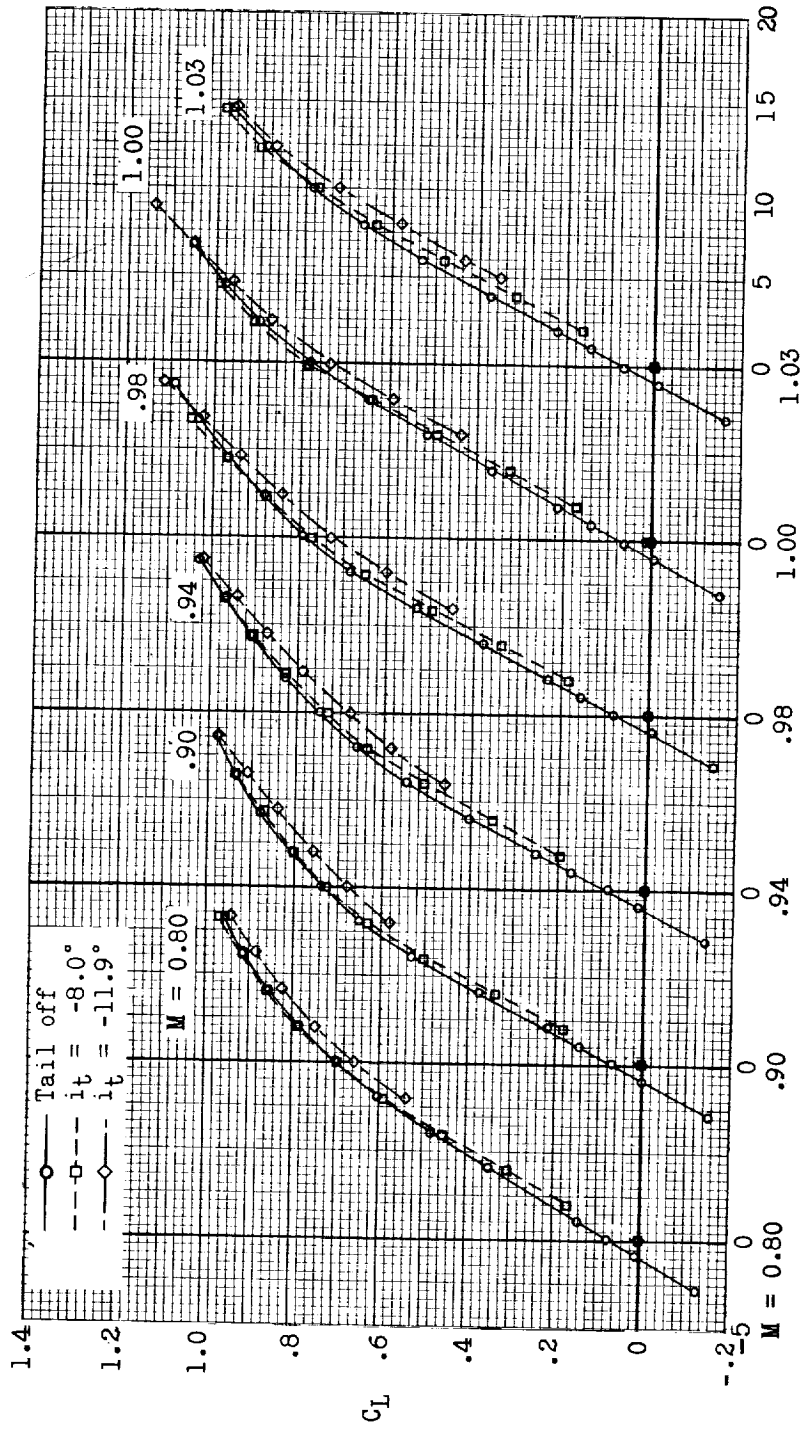

(a) Concluded.

Figure 3.- Continued.

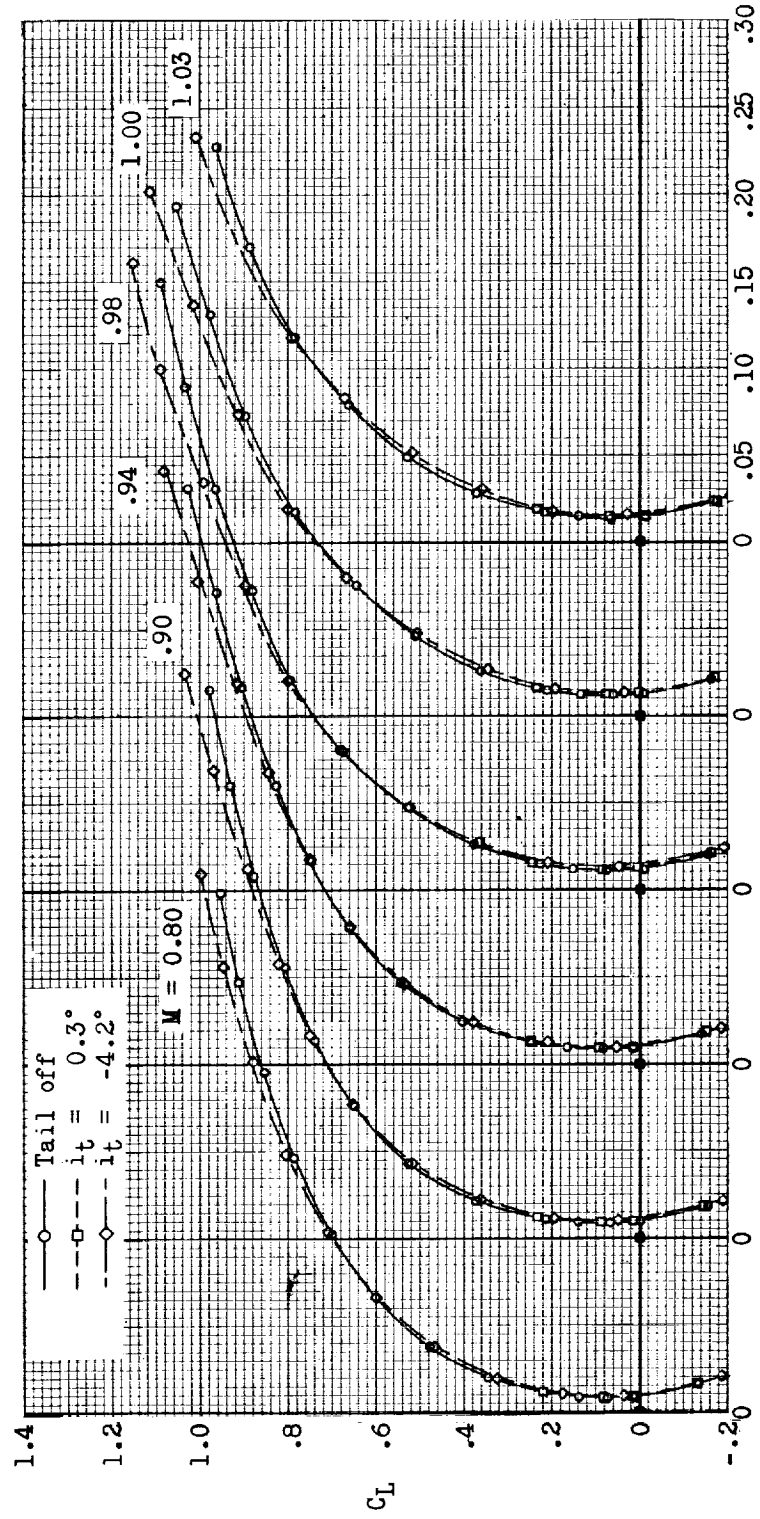

(b) Variation of C_L with C_D.

Figure 3.- Continued.

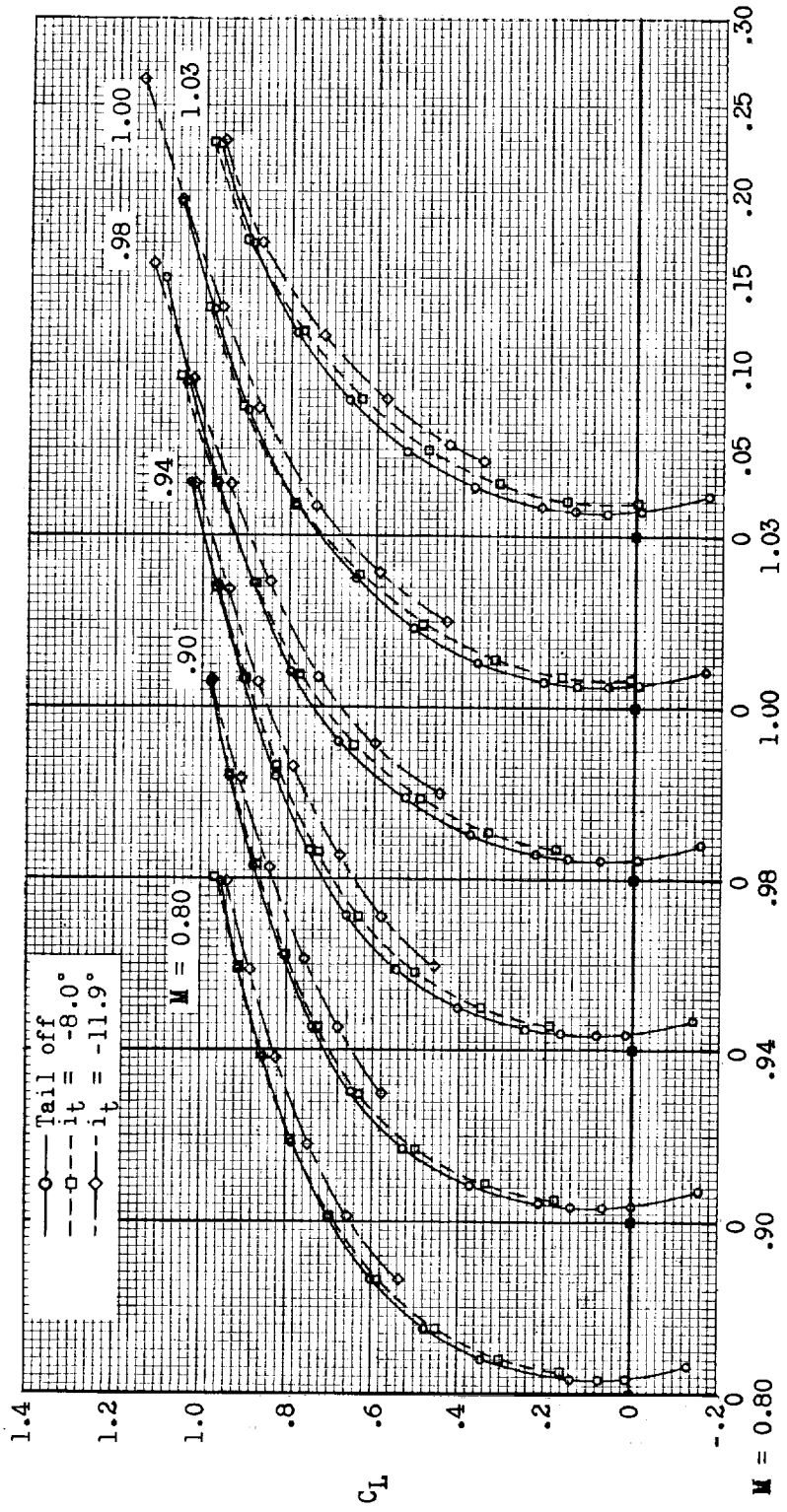

(b) Concluded.

Figure 3.- Continued.

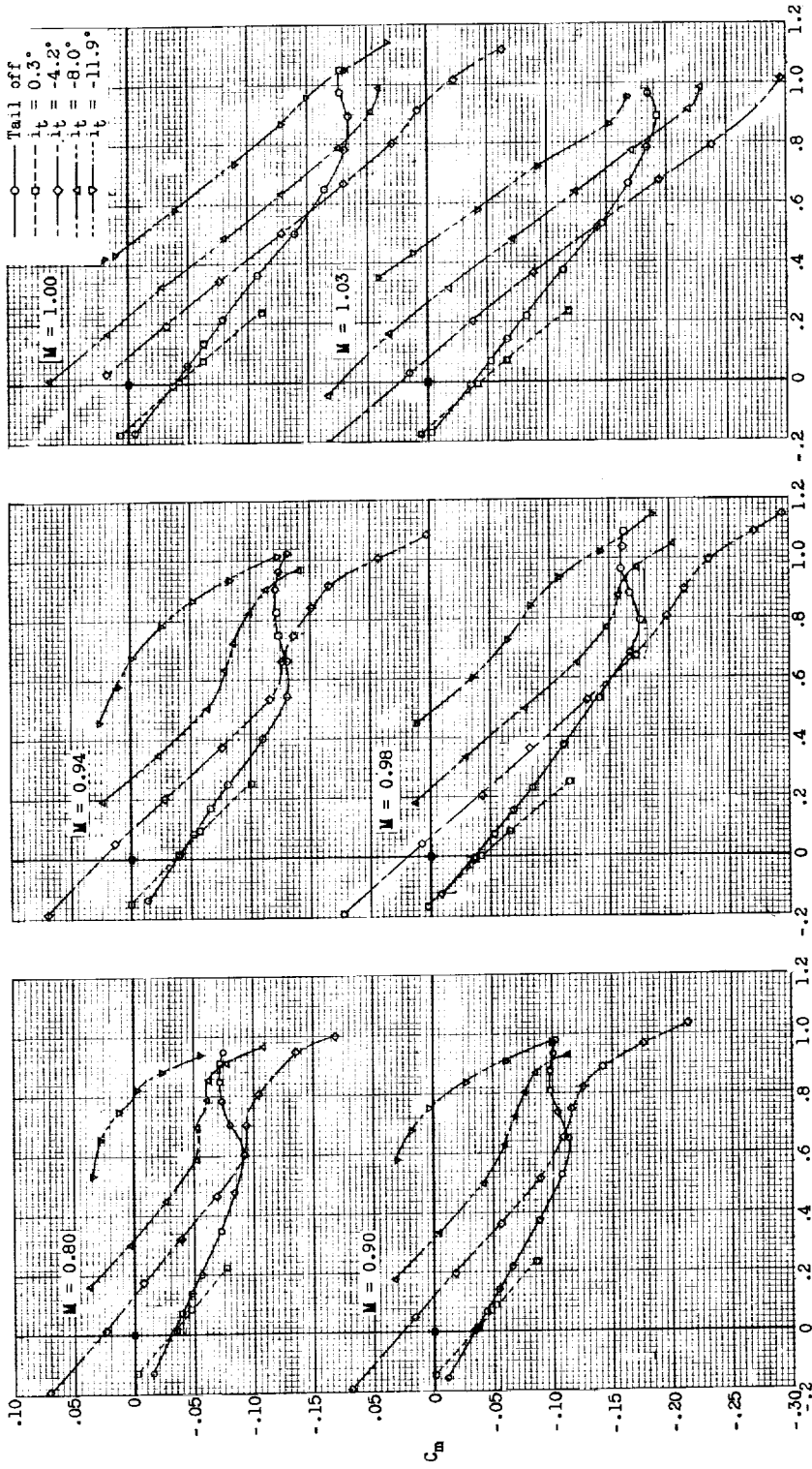

(c) Variation of C_m with C_L.

Figure 3.- Continued.

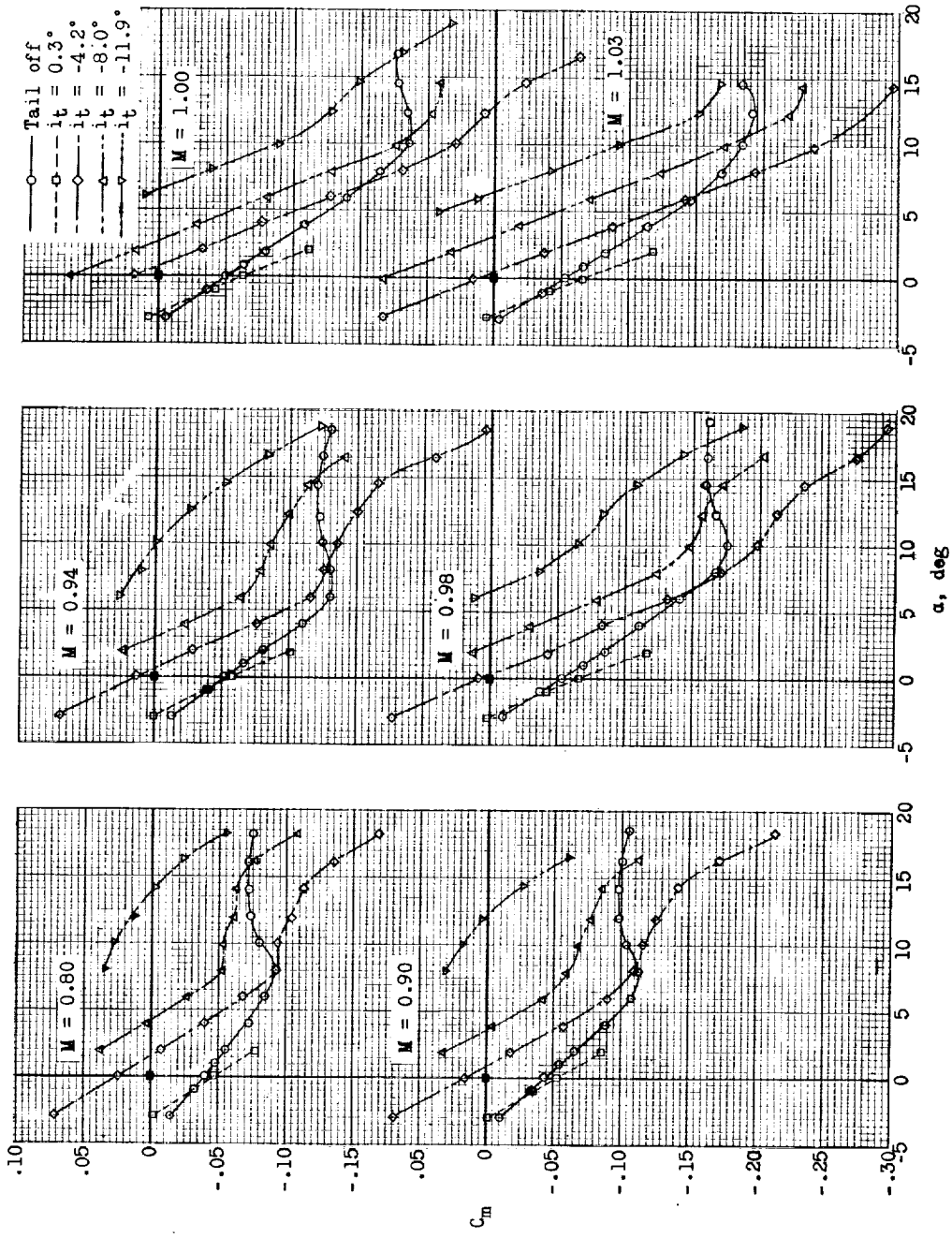

(d) Variation of C_m with α.

Figure 3.- Concluded.

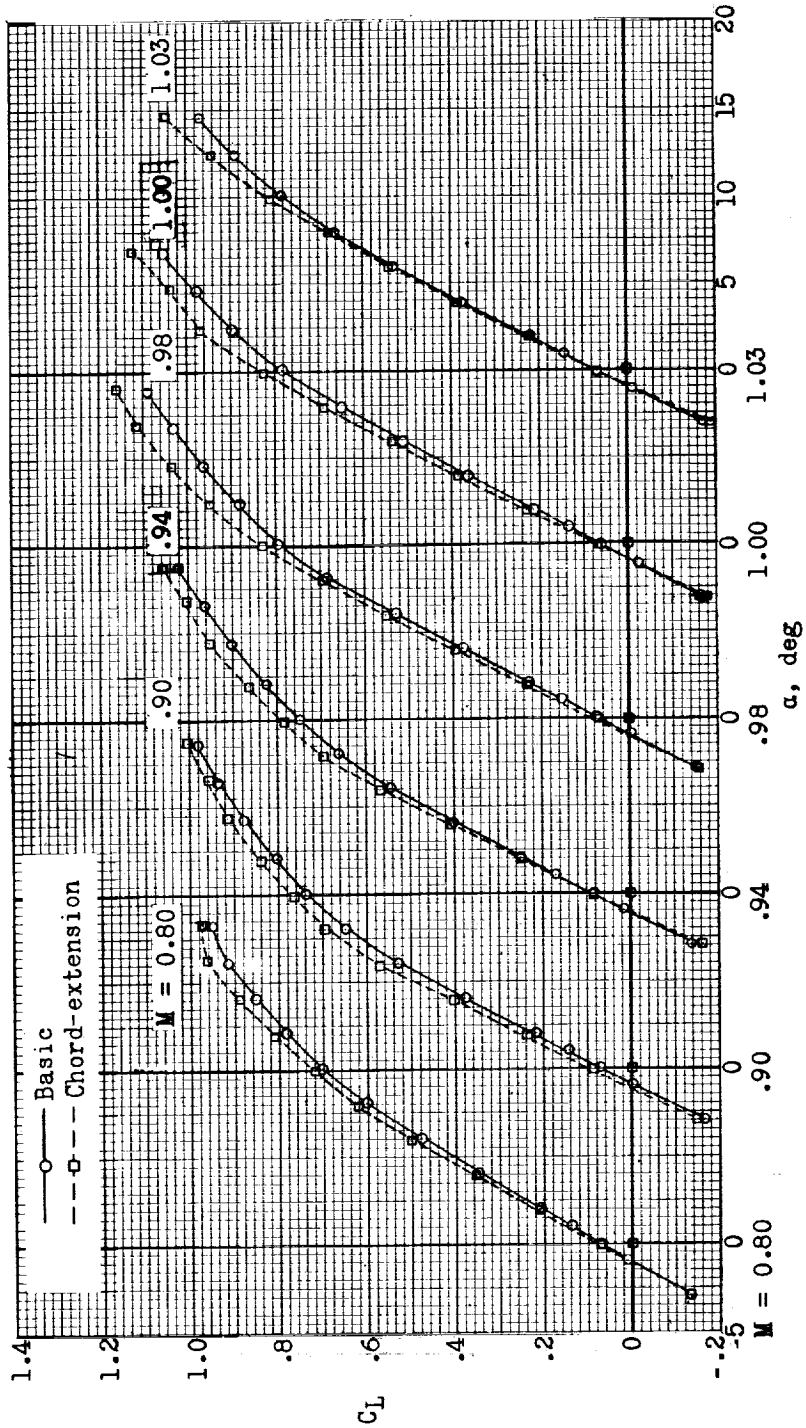

(a) Variation of C_L with α.

Figure 4.- Longitudinal aerodynamic characteristics for basic and leading-edge chord-extension configurations. Tail off.

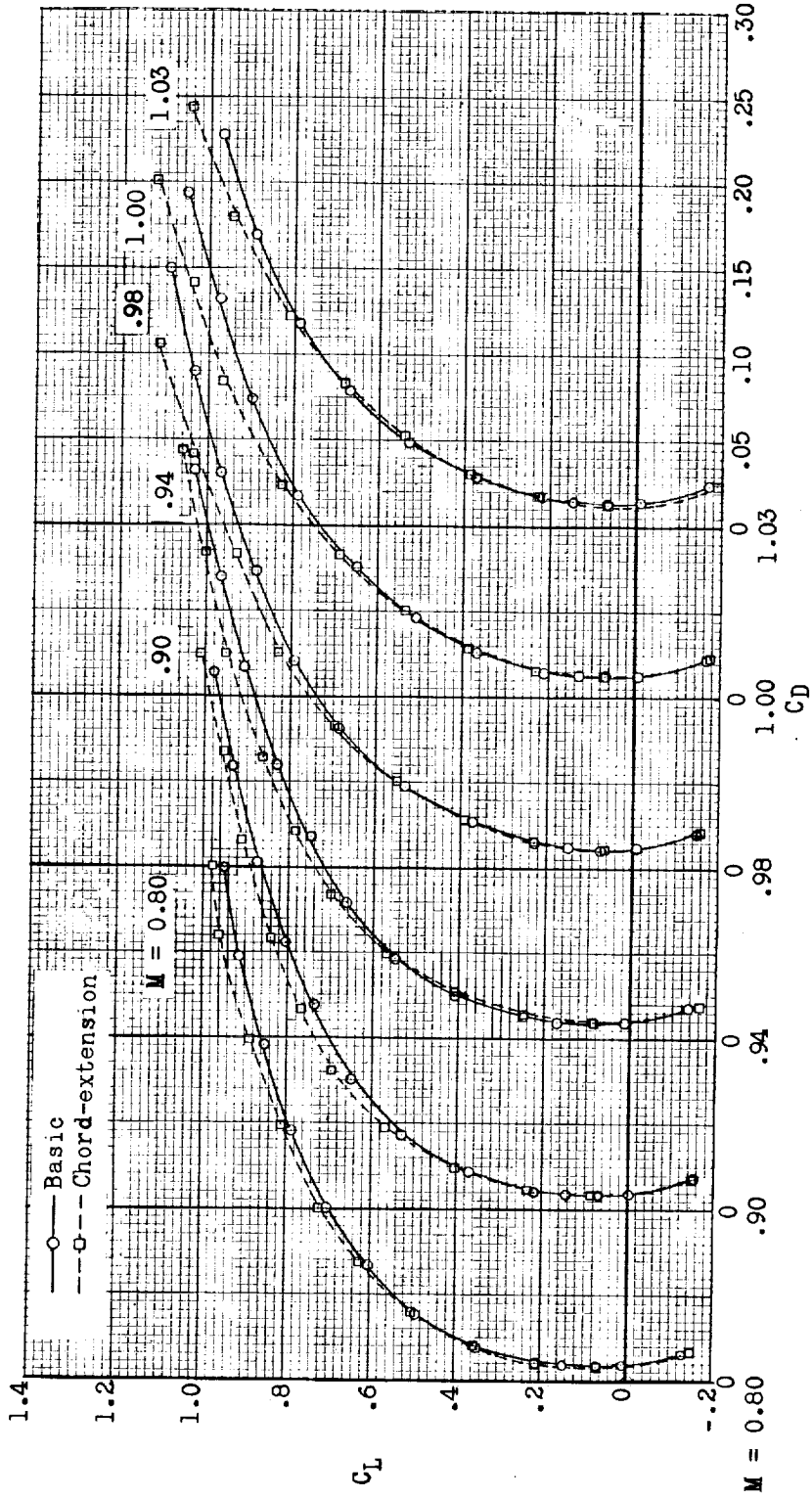

(b) Variation of C_L with C_D.

Figure 4.- Continued.

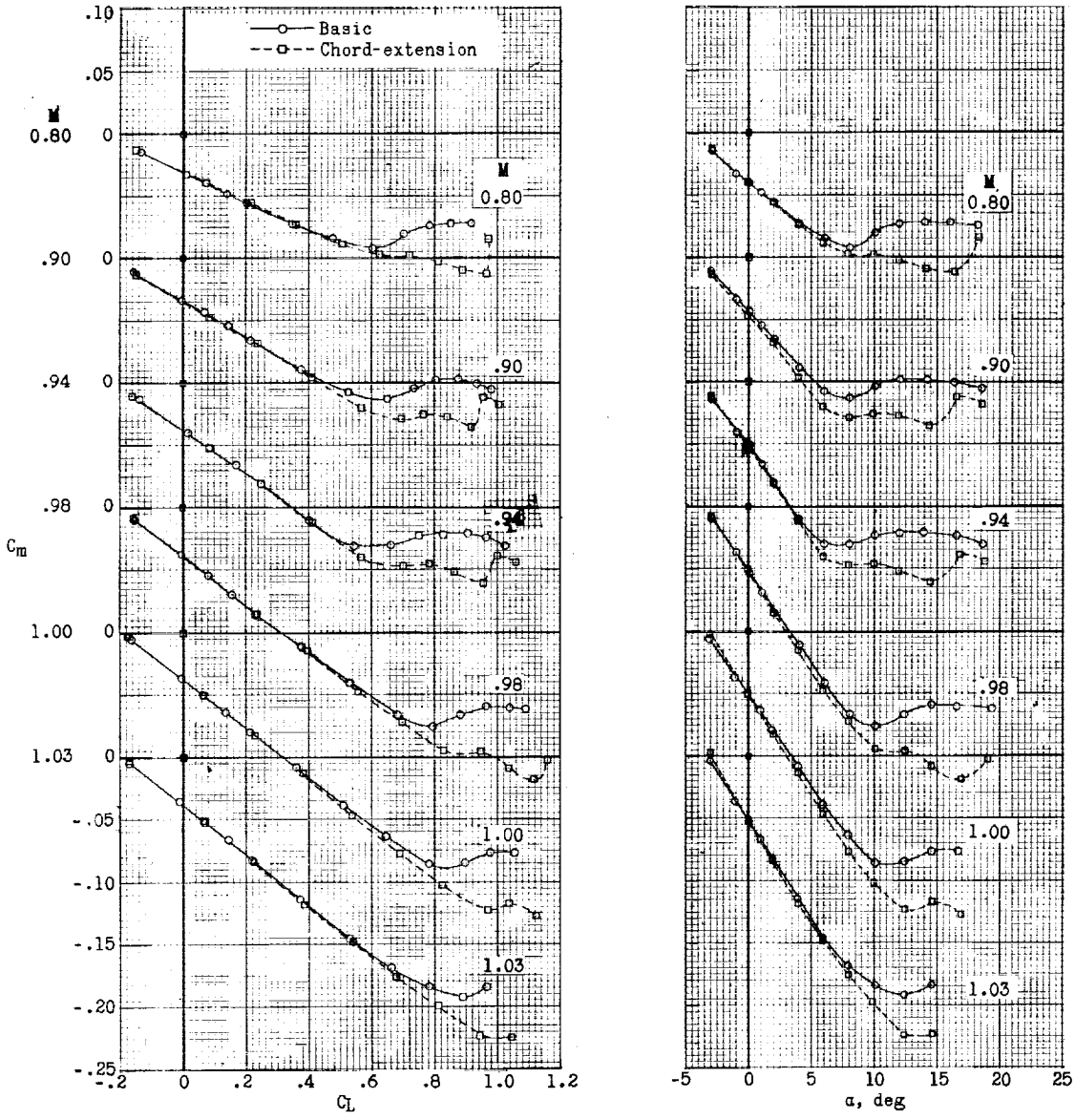

(c) Variation of C_m with C_L. (d) Variation of C_m with α.

Figure 4.- Concluded.

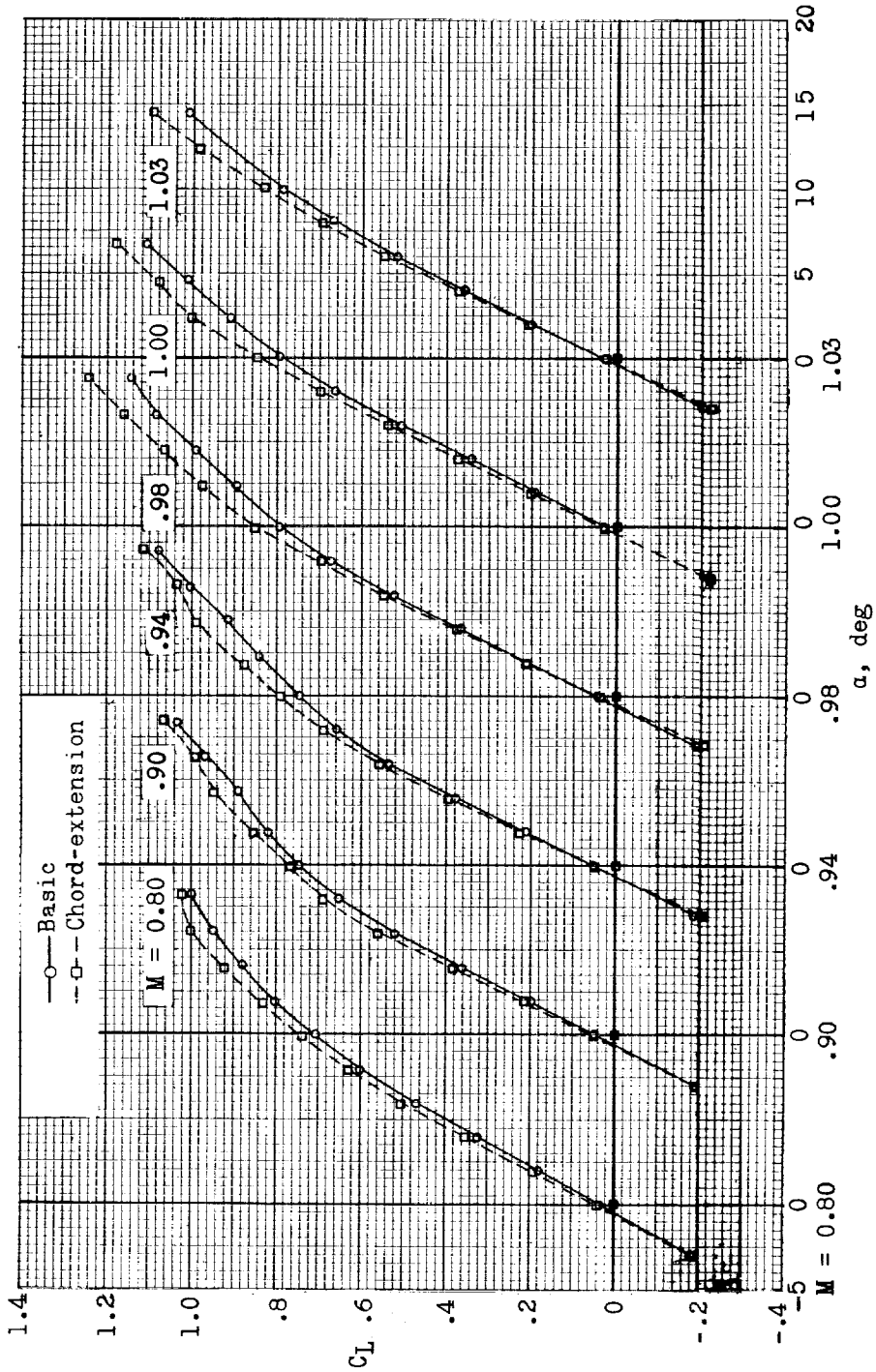

(a) Variation of C_L with α.

Figure 5.- Longitudinal aerodynamic characteristics for basic and leading-edge chord-extension configurations. Tail on; $i_t = -4.2°$.

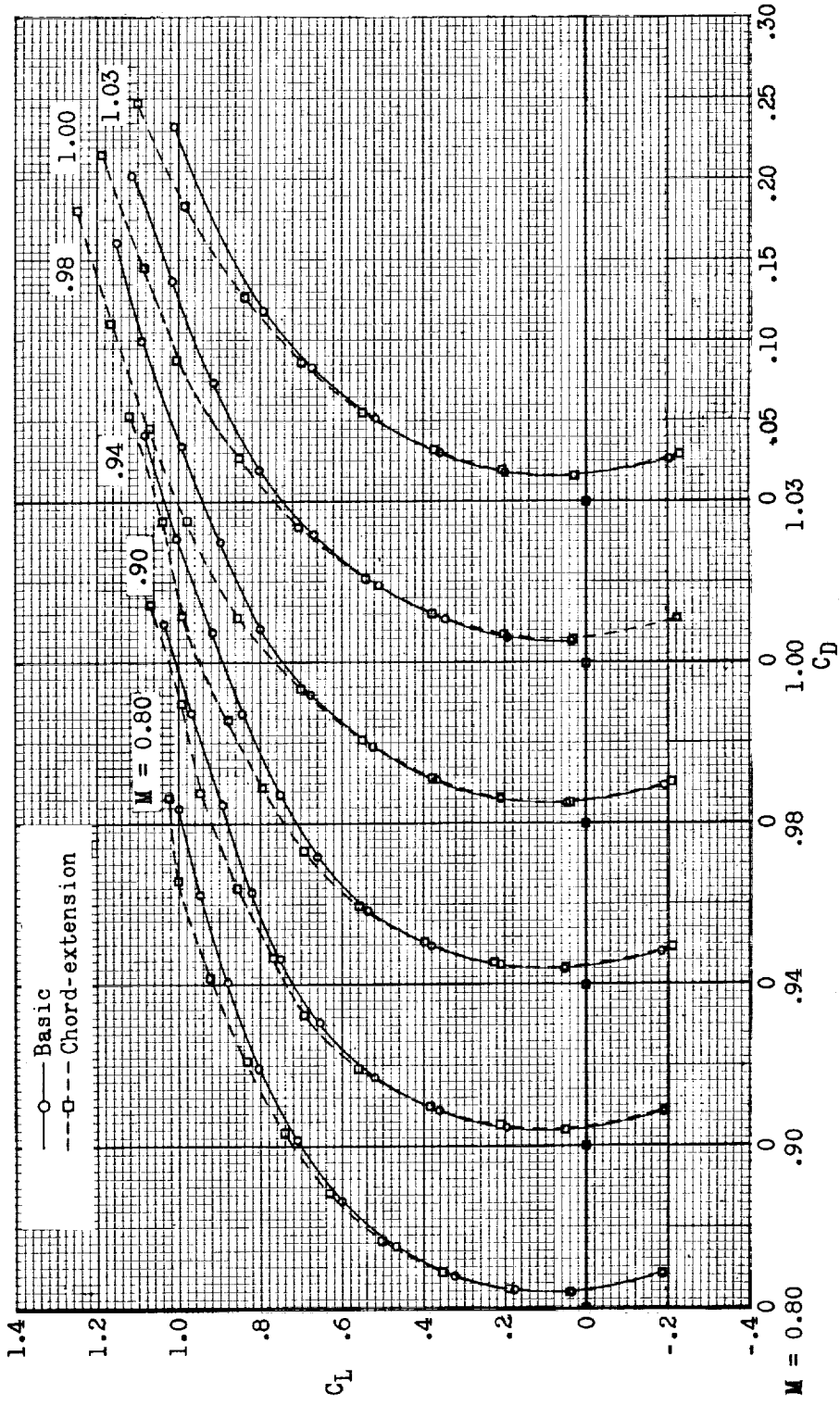

(b) Variation of C_L with C_D.

Figure 5.- Continued.

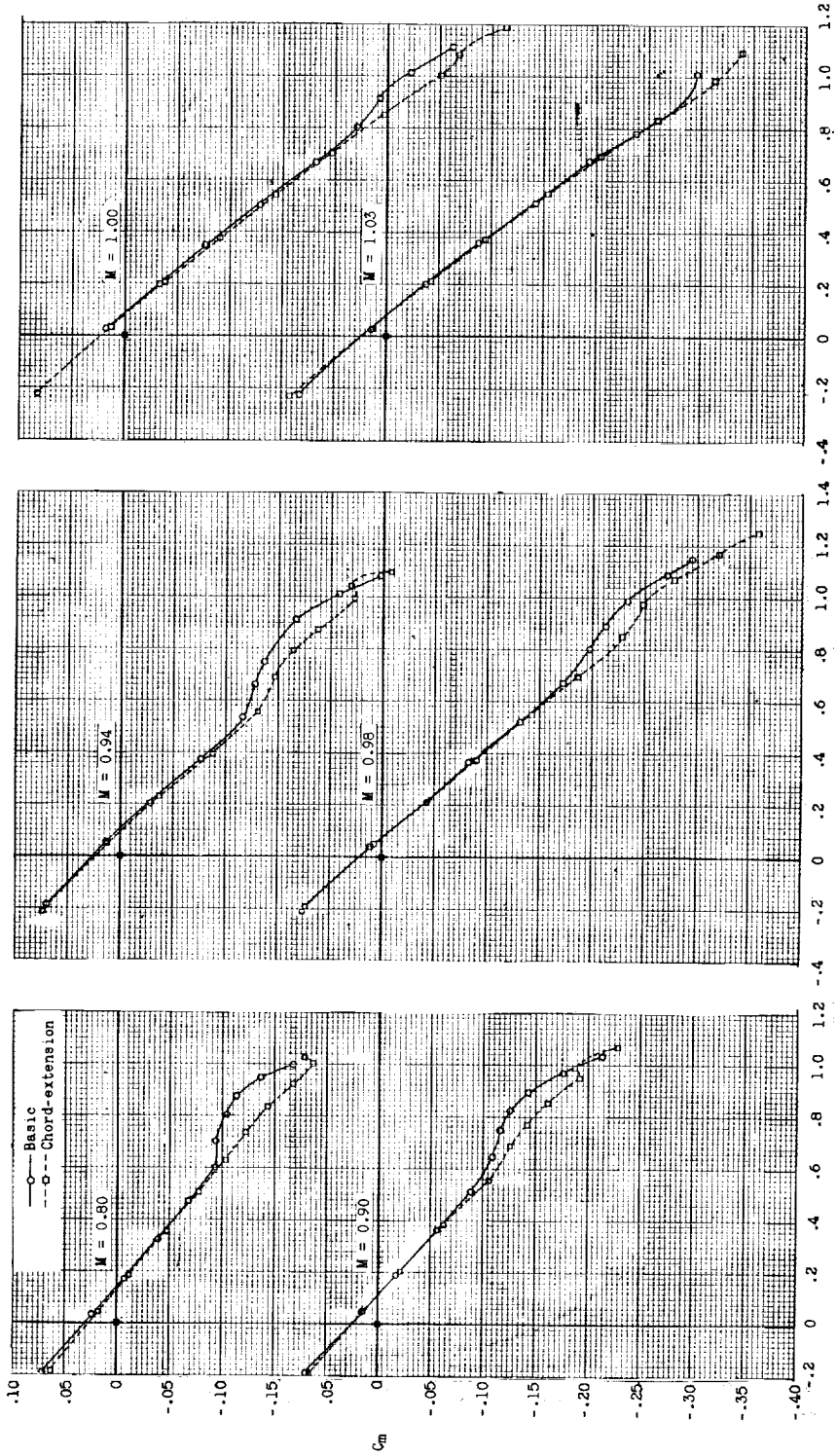

(c) Variation of C_m with C_L.

Figure 5.- Continued.

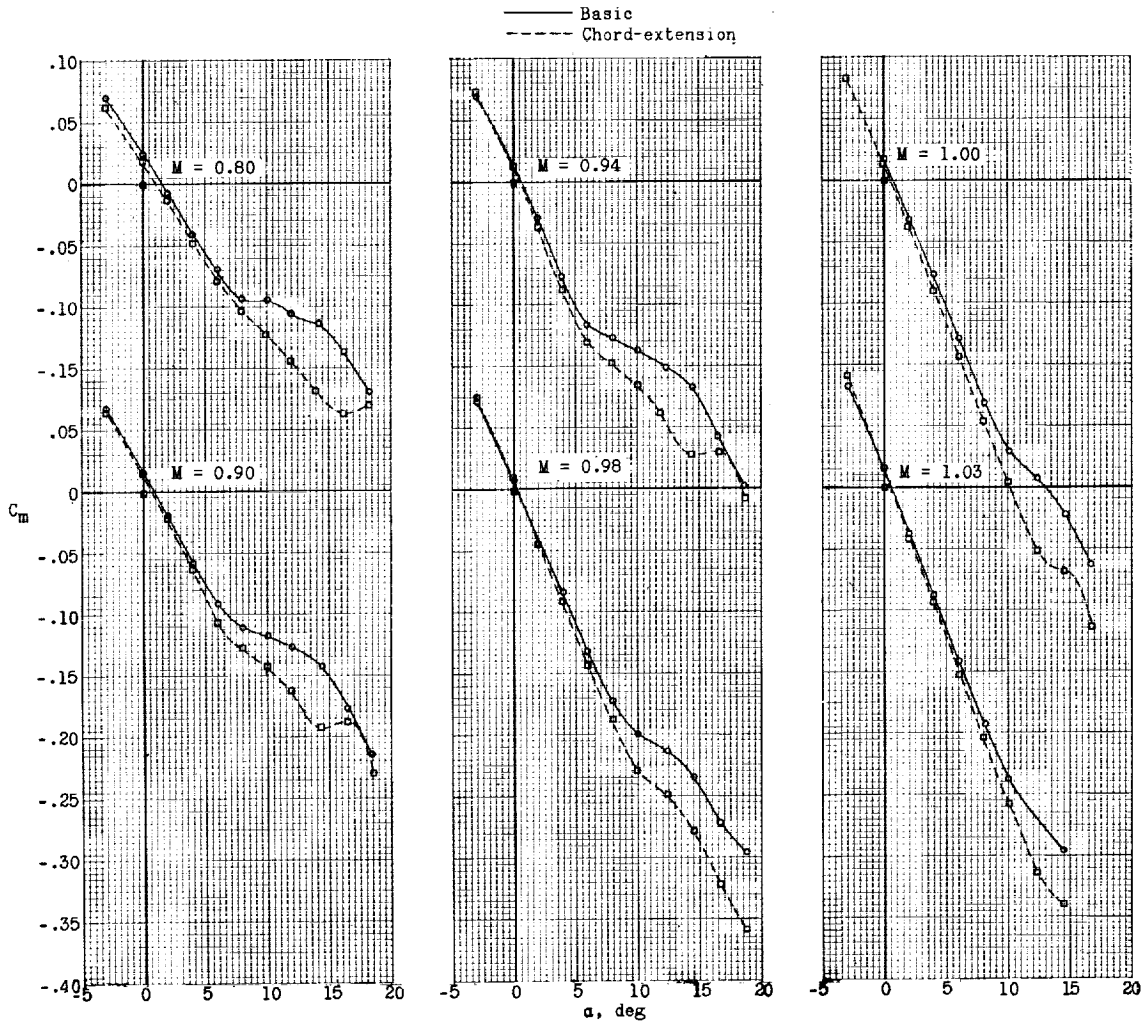

(d) Variation of C_m with α.

Figure 5.- Concluded.

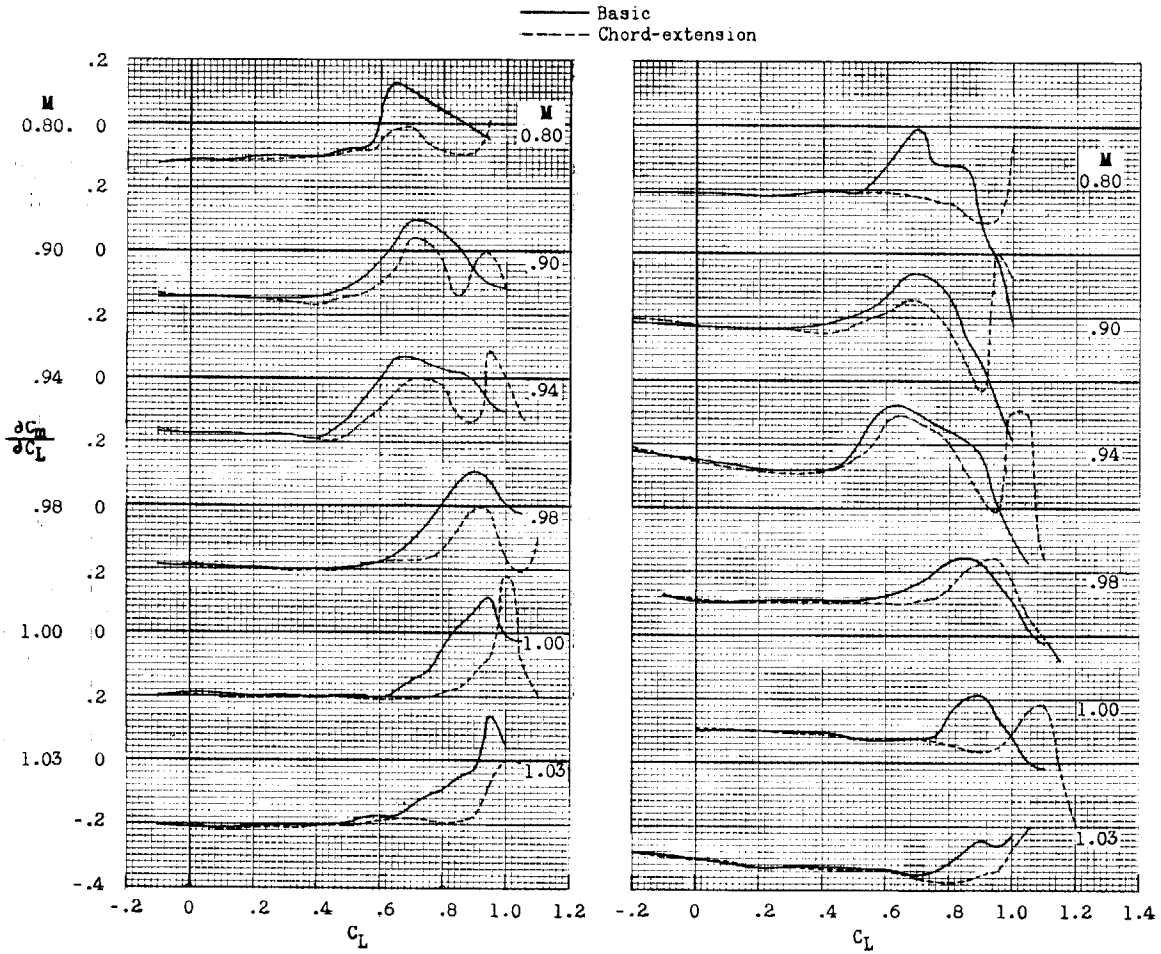

(a) Tail off.

(b) $i_t = -4.2^\circ$.

Figure 6.- Variation of longitudinal-stability parameter with lift coefficient for basic and leading-edge chord-extension configurations.

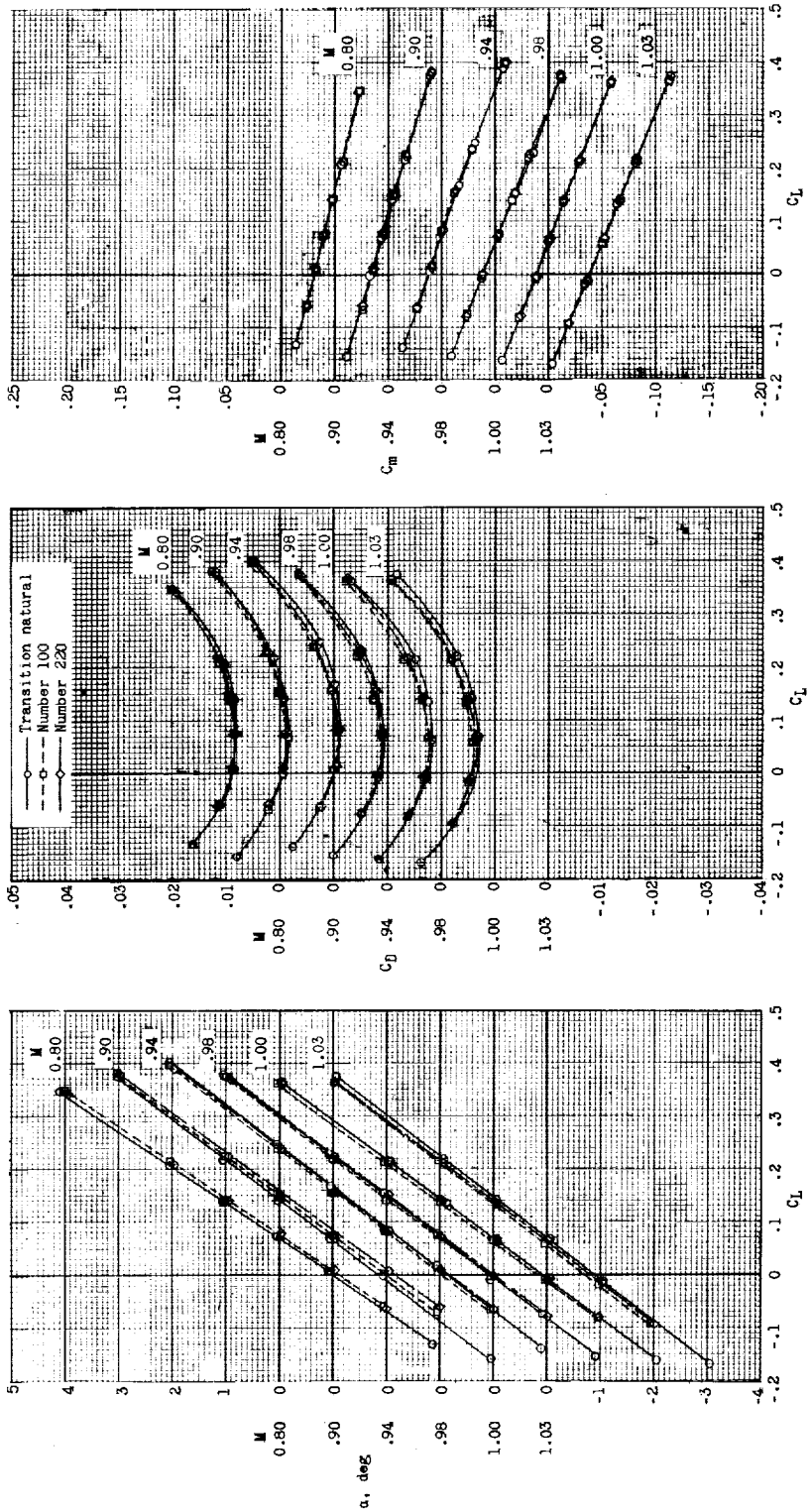

(a) Variation of α with C_L.

(b) Variation of C_D with C_L.

(c) Variation of C_m with C_L.

Figure 7.- Effect of transition strips on longitudinal aerodynamic characteristics of basic configuration. Tail off.

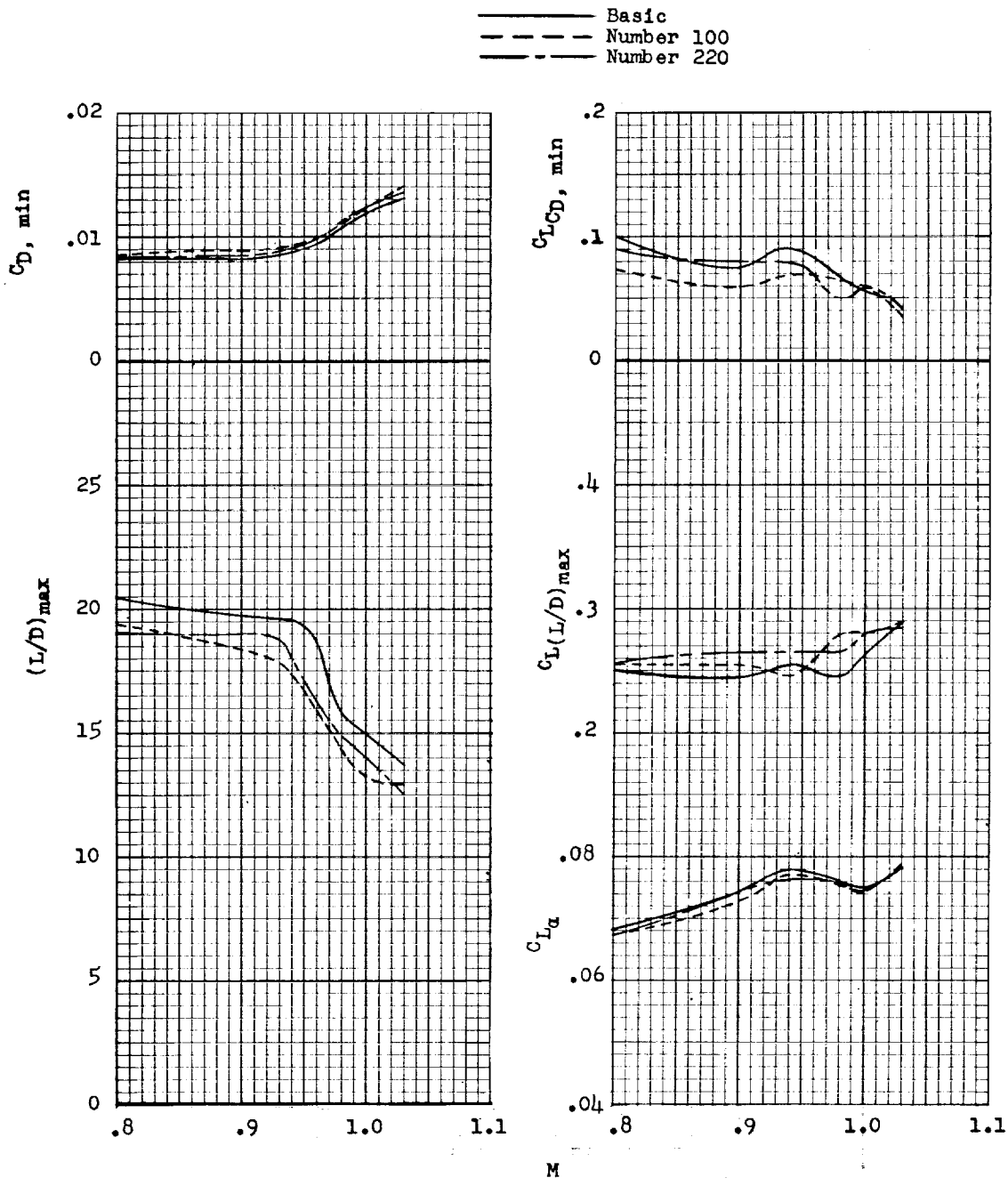

Figure 8.- Effect of transition strips on variation of minimum drag coefficient, maximum lift-drag ratio, corresponding lift coefficients, and lift-curve slope with Mach number for basic configuration. Tail off.

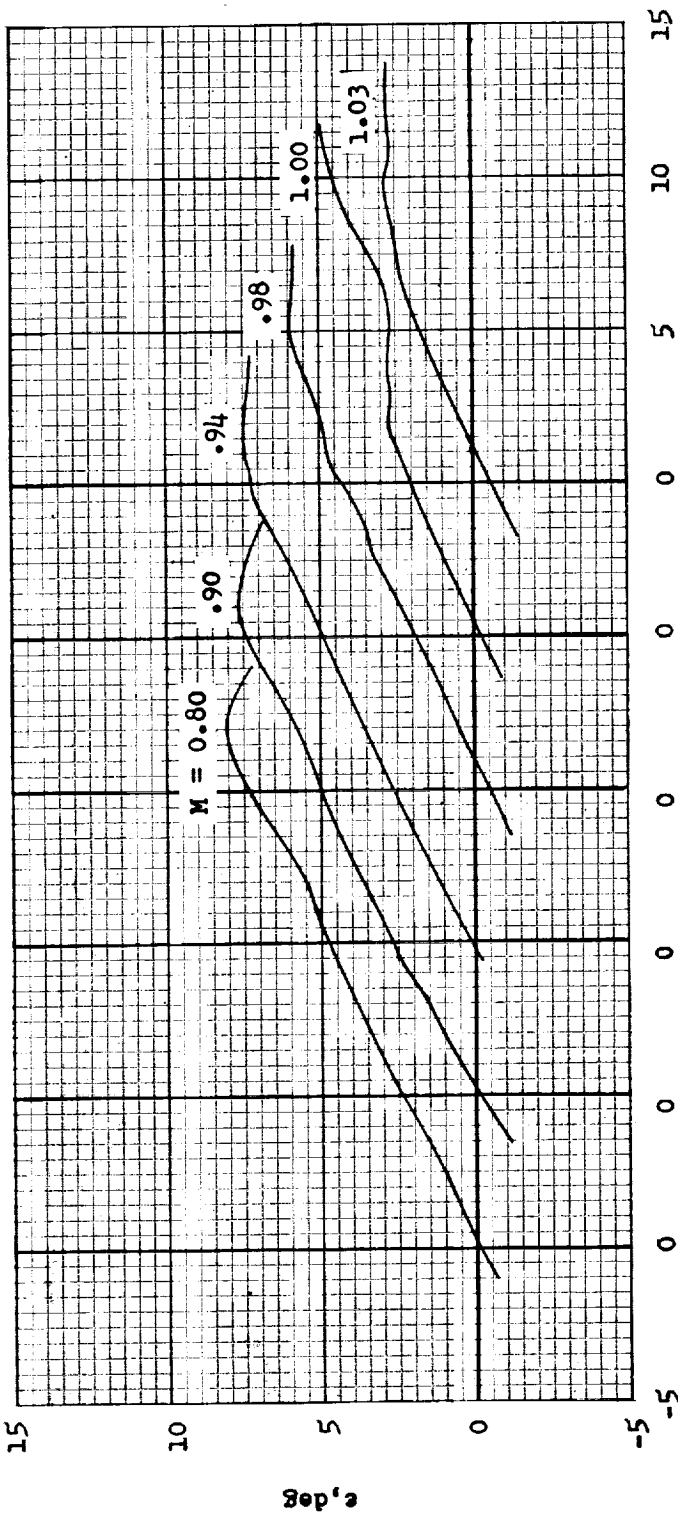

Figure 9.- Variation of effective downwash angle with angle of attack for basic configuration.

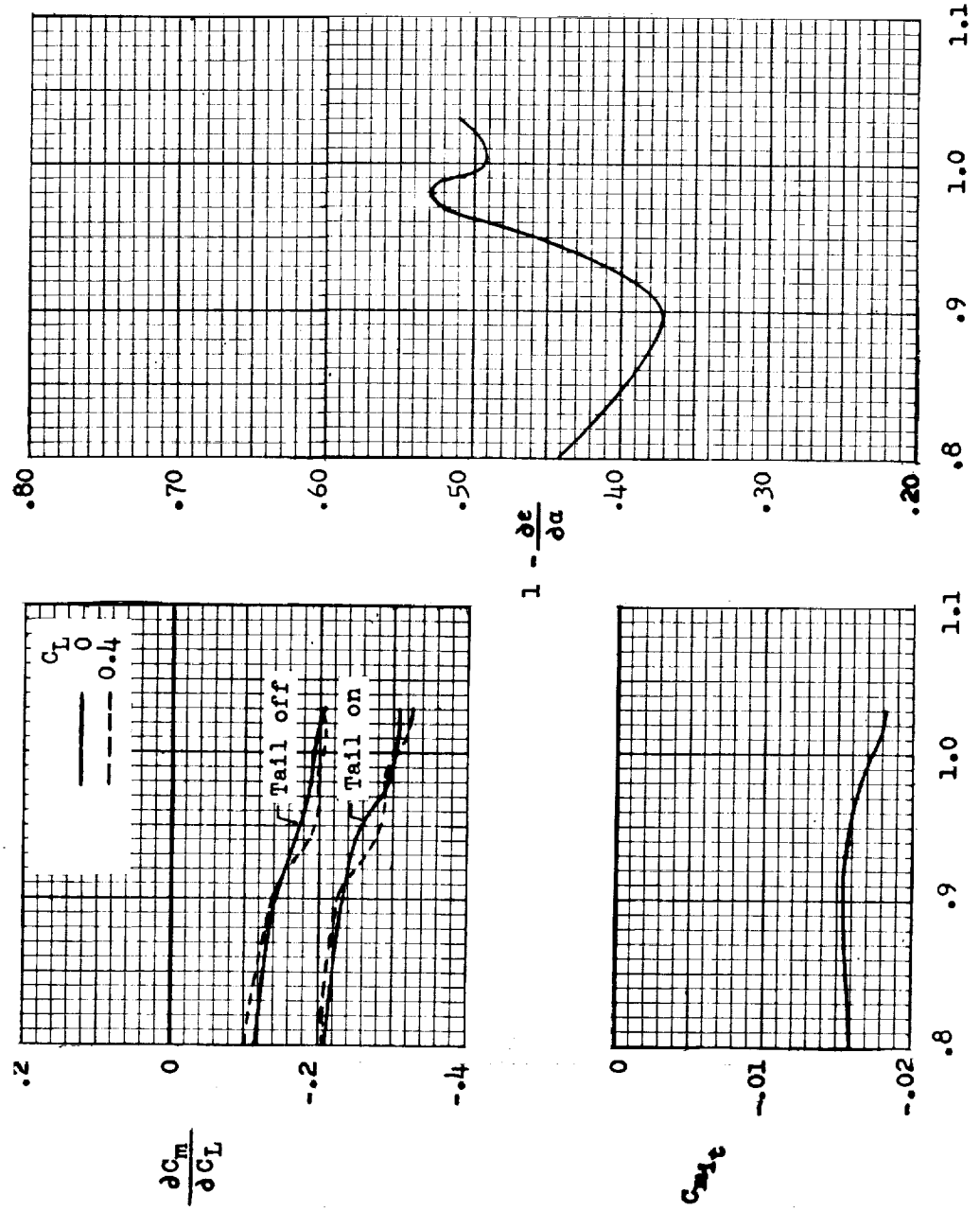

Figure 10.- Variation of longitudinal-stability, tail-effectiveness, and downwash parameters with Mach number for basic configuration.

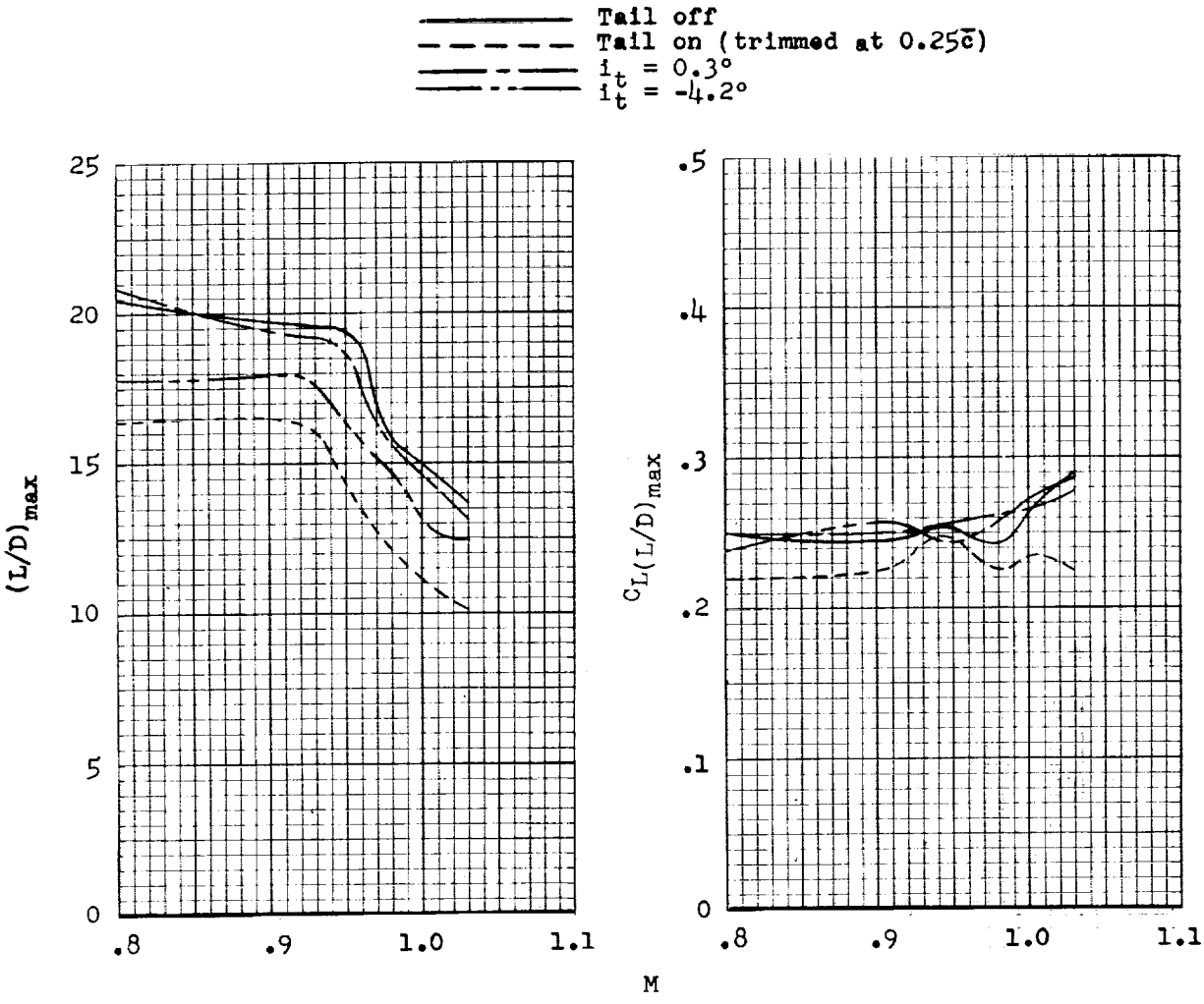

Figure 11.- Comparison of variation of maximum lift-drag ratio and lift coefficient for maximum lift-drag ratio with Mach number for basic configuration with and without tail.

NASA - Langley Field, Va. L-462